Supplementary Information for

Ruling out Delamination and Bismuth-enhanced Polyimide Electrochemical Actuator with Tunable Active/Passive Layer Thickness

Si-Qi Wang[a], Bin Zhang[a,*], Xue-Mei Luo[b], Fei Liang[b], Guang-Ping Zhang[b,*]

**To whom correspondence should be addressed: zhangb@atm.neu.edu.cn; gpzhang@imr.ac.cn*

[a] *Key Laboratory for Anisotropy and Texture of Materials, Ministry of Education, School of Materials Science and Engineering, Northeastern University, 3-11 Wenhua Road, Shenyang 110819, P. R. China*

[b] *Shenyang National Laboratory for Materials Science, Institute of Metal Research, Chinese Academy of Sciences, 72 Wenhua Road, Shenyang 110016, P. R. China*

A typical surface morphology of a sandpaper scratched PI film was characterized by using laser confocal scanning microscopy, which is shown in Fig. S1. The average value of five times measurement of the root-mean-square roughness of the roughed surface was 0.337 μm.

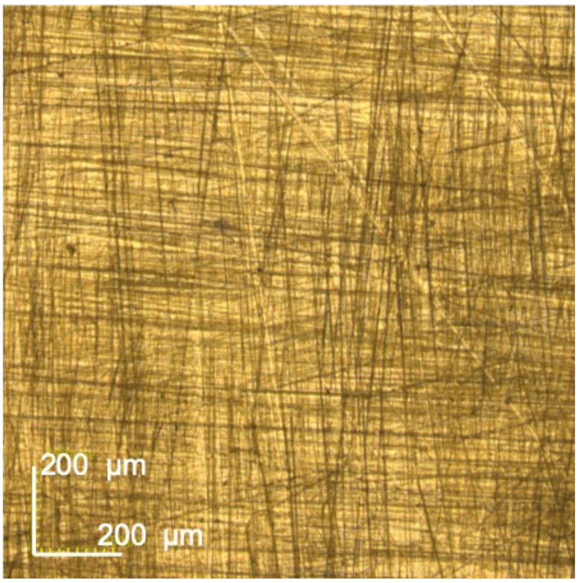

Fig S1. Surface LCSM image of sandpaper roughed PI film.

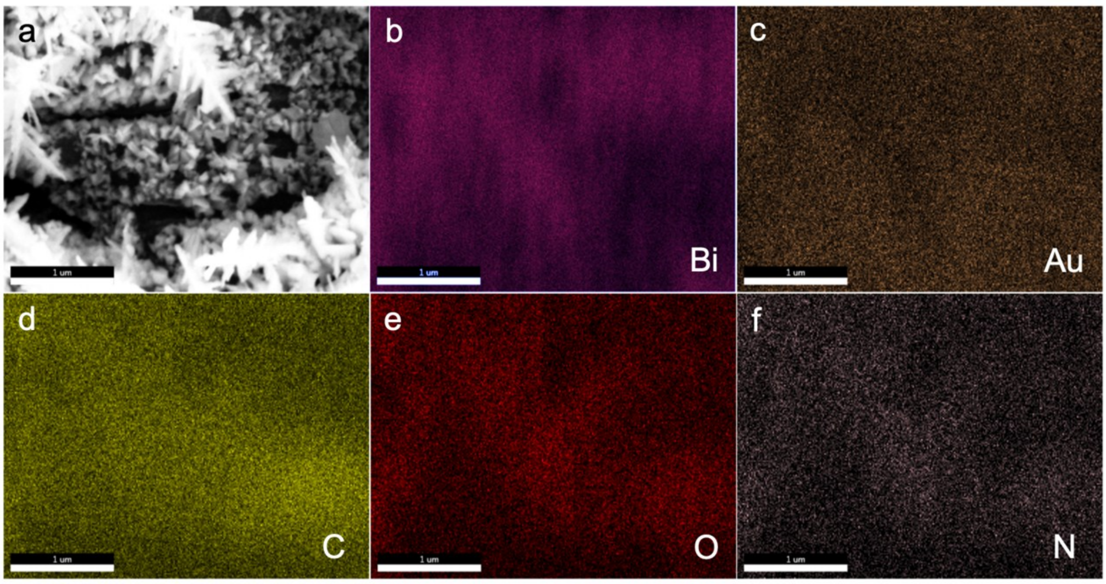

Fig S2. Energy dispersive X-Ray spectroscopy (EDS) elemental mapping images of as-fabricated PI/Au/Bi film, a) SEM image; b, c, d, e and f) Element distribution of Bi, Au, C, O and N, respectively.

Characterization of film thickness

The thickness of the Bi layer is about 3 μm which can be seen clearly in LCSM image and the corresponding height profile lines shown in Fig S3. The total thickness of the PI/Au/Bi film is about 28.3 μm, thus the thickness of the Au layer should be 0.3 μm.

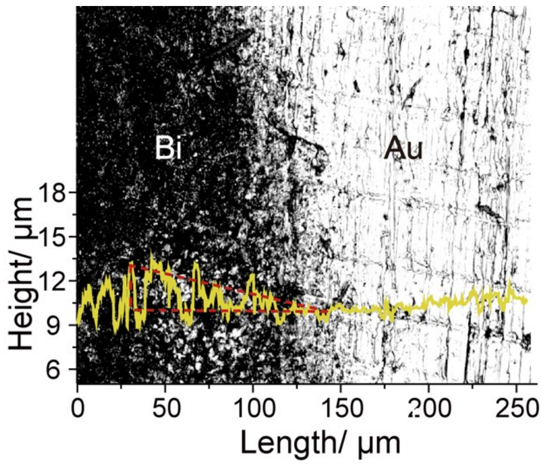

Fig S3. LCSM image of interface area between Au and Bi (inset shows the corresponding height profile line).

Calculation of actuation strain

Due to the mechanism of actuating in this work is the volume expansion of the active PI layer and the constraint of the passive PI layer, the calculation of the strain ignoring the thickness of Au and Bi layers following a simplified calculation model reported by Kwan et al.[S1]

First, a simple rectangular plane coordinate system was set up shown in Figure S4a. The thickness of the active and passive PI layers is represented by t_a and t_p, respectively. When voltage stimulation is supplied, the active PI layer will expand due to the insertion of the K^+ and water molecules, and the entire film bended towards the direction of the passive layer (see Figure S4b). If the active layer is freed from the passive layer, the active PI will elongate uniformly as shown in Figure S4c. In this condition, the stress of the active layer is zero, and the intrinsic strain of active layer is ε_i. Actually, the strain of the whole actuator (ε) consist of uniform elongation strain component c and bending strain component $\frac{z - t_0}{R}$, that is,

$$\varepsilon = c + \frac{z - t_0}{R}, \; (- t_p \leq z \leq t_a) \tag{S1}$$

where t_0 is the position of bending axis where the bending strain component c is zero. R stands for the radius of curvature calculated by the position of free end P (a, b),

$$R = \frac{a^2 + b^2}{2a} \tag{S2}$$

For the large deformation, radius of curvature was received by circle fitting model and standard by scale.

As the specific state of the actuator is in equilibrium, three boundary conditions are appropriate. First, the force derived from uniform elongation strain within the material is zero:

$$E_p t_p c + E_a t_a (c - \varepsilon_i) = 0 \tag{S3}$$

where E_p and E_a are taken as the elastic modulus of the passive layer and the active layer, respectively. Here we treat them as equal. Secondly, the force due to the bending strain within the material is zero:

$$\int_{-t_p}^{0} \frac{E_p(z - t_0)}{R} \mathrm{dz} + \int_{0}^{t_a} \frac{E_a(z - t_0)}{R} \mathrm{dz} = 0 \qquad (S4)$$

Thirdly, the sum of the bending moment relative to the bending axis is zero:

$$\int_{-t_p}^{0} \left(z - t_0\right) E_s \varepsilon \, \mathrm{d}z + \int_{0}^{t_a} (z - t_0) E_a (\varepsilon - \varepsilon_i) = 0 \tag{S5}$$

Solving these boundary conditions gives that:

$$\varepsilon_i = \frac{1}{6R\left(t_a + t_p\right)} \left[\frac{t_a^3}{t_p} + \frac{t_p^3}{t_a} + 4(t_a^2 + t_p^2 + 1.5 t_a t_p)\right] \tag{S6}$$

For the intrinsic strain of PI/Au/Bi under −1 V voltage stimulation after 60 s, where

R=1.25 mm,

$t_a + t_p = 0.025$ mm,

$t_a = 0.0008$ mm,

$t_p = 0.025$ mm–0.0008 mm = 0.0242 mm,

$$\varepsilon_{60\,s} = \frac{1}{6 \times 1.25 \times 0.025} \left(\frac{0.0008^3}{0.0242} + \frac{0.0242^3}{0.0008} + 4 \times (0.0008^2 + 0.0242^2) + 1.5 \times 0.0008 \right.$$

=10.8%

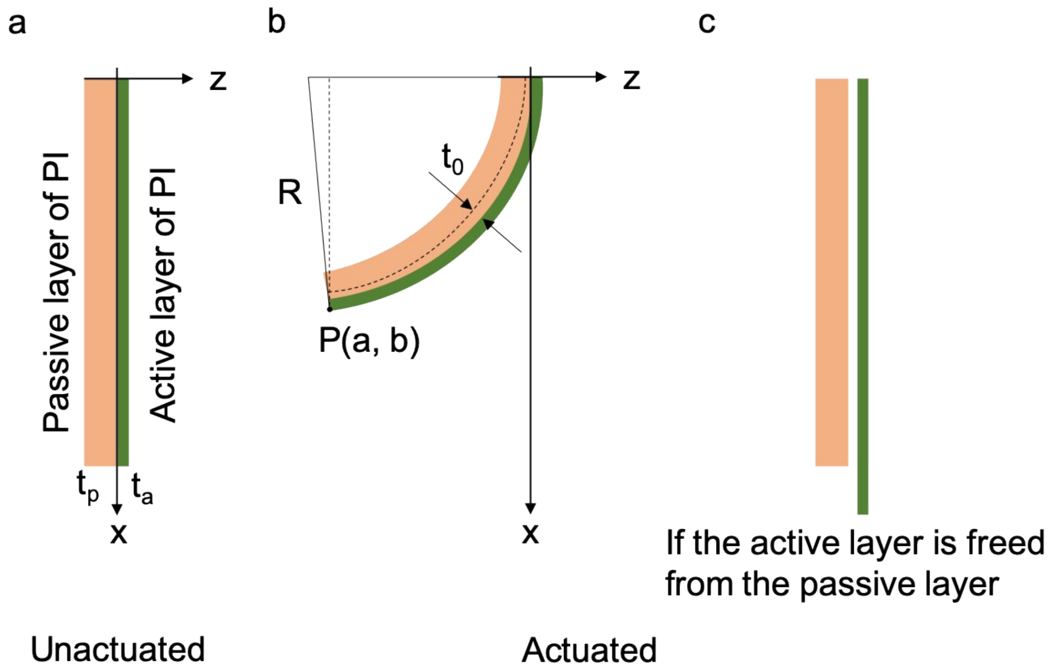

Fig S4. Schematic diagram for calculation of actuating strain of PI active layer in PI/Au/Bi film. a) Unactuated state of PI, b) Real actuated state of PI, and c) Actuated state if the active layer (green) of PI is freed from the passive layer (orange).

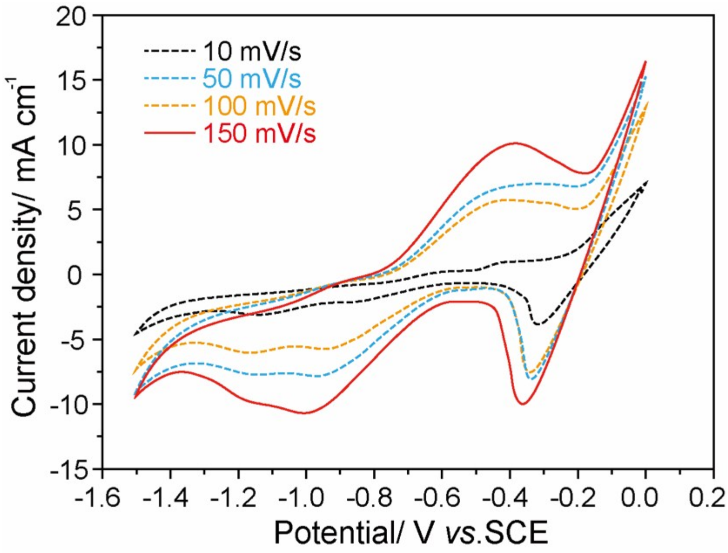

Fig S5. CV curves of PI/Au/Bi films at scan rates of 10, 50, 100, 150 mV s^{-1}, respectively.

SEM observation of actuator after cyclic loading

Fig S6a shows a typicl morphology of the surface Bi film of an actuator after 5×10^3 cyclic test. No obvious morphology change and structural collape happened on the actuator even after 5×10^3 cyclic test except for few dendrites falling out. Notably, the dark furrow, shown in Fig S6a, produced by the sandpaper scratch in the previous fabrication process was also observed carefully and shown in Fig S6b. The desely distributed particles indicate the structual stability of the surface Bi film even after 5×10^3 cyclic loading, and what is more, almost all the dark area shown in the lower-magnification SEM image were fully covered by the Bi.

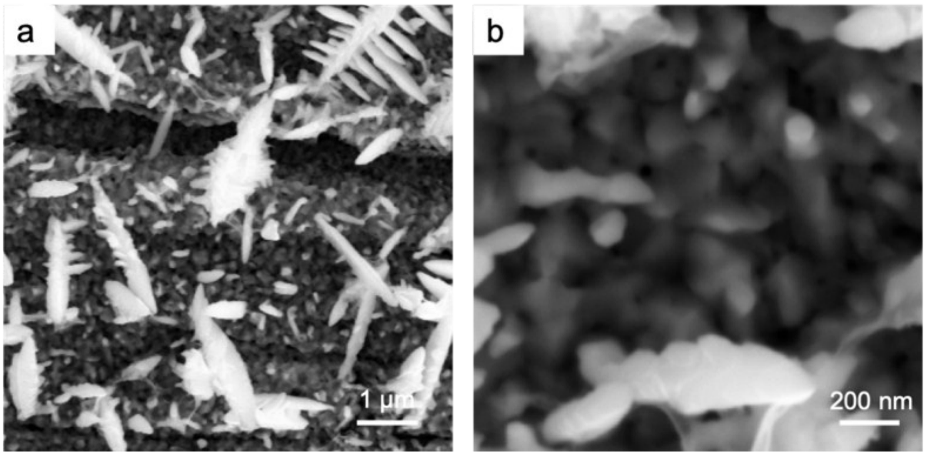

Fig S6. SEM images of surface Bi film of an actuator after 5×10^3 cycles testing a) observed at lower magnification, and b) zoomed in at the dark furrow shown in Fig S7a.

Table S1. Comparison of actuation performance of different actuators

Actuating Material	Maximum Strain	Response Speed	Potential Window	Cycle life	References
$Ni(OH)_2/NiOOH@Ni$ in 1 M NaOH	0.16%	2.3°/s	0~0.425 V vs. SCE	High stability (500th)	S2
MoS_2@Au@kapton in 0.5 M H_2SO_4	0.8%	0.0067%/s	-0.3~0.3 V vs. SCE	Stable continuous actuation for three days	S3
MnO_2@Ni film in 0.5 M Na_2SO_4	0.3%	0.008%/s	0~1 V vs. SCE	77.3% (1000 th)	S4
non-volatile LixGe/PI/LixGe	8.2%	0.9 mm/s	2 V	43% (100 th)	S5
Sulfonated Polyimide/silver	Displacement of 1.12 mm	1°/s	0.5 V dc	/	S6
BS-COF-C900/PEDOT：PSS	0.62%	0.124%/s	±0.5 V ac	90% (6 h)	S7
This work	**10.8%**	**10°/s 0.18%/s**	**-1~0 V vs. SCE**	**94% (5000th)**	

Tensile test

To evaluate the mechanical strength of the PI/Au/Bi actuators, tensile test was conducted using three rectangular PI/Au/Bi films with dimensions of 10 mm×3, and the total thickness is 28.3 μm. The average yield strength (elastic limit stress) and the ultimate strength of the films are 77 MPa and 118 MPa, respectively. Fig S7 shows a typical stress-strain curve.

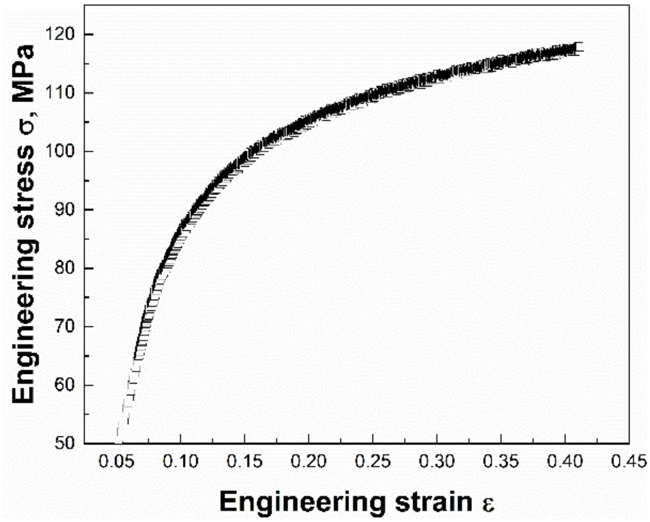

Fig S7 The engineering stress-strain curve of a PI/Au/Bi film

S1 K. W. Kwan, S. J. Li, N. Y. Hau, W. Di Li, S. P. Feng and A. H. W. Ngan, *Sci. Robot.*, 2018, **3**, eaat4051.

S2 K. W. Kwan, N. Y. Hau, S. P. Feng and A. H. W. Ngan, *Sensors Actuators, B Chem.*, 2017, **248**, 657-664.

S3 M. Acerce, E. K. Akdoğan and M. Chhowalla, *Nature*, 2017, **549**, 370.

S4 L. Liu, L. Su, Y. Lu, Q. Zhang, L. Zhang, S. Lei, S. Shi, M. D. Levi and X. Yan, *Adv. Funct. Mater.*, 2019, 1806778.

S5 M. S. Noh, H. Lee, Y. G. Song, I. Jung, R. Ning, S. W. Paek, H. C. Song, S. H. Baek, C. Y. Kang and S. Kim, *Nano Energy*, 2019, **57**, 653-659.

S6 J. Song, J. H. Jeon, I. K. Oh and K. C. Park, *Macromol. Rapid Commun.*, 2011, **32**, 1583-1587.

S7 S. Roy, J. Kim, M. Kotal, R. Tabassian, K. J. Kim and I. K. Oh, *Adv. Funct. Mater.*, 2019, **29**, 1900161.